Pediatric Cardiology (2023) 44:1382–1396
https://doi.org/10.1007/s00246-023-03131-y

RESEARCH

Speckle Tracking Analysis in Fetuses with D-Transposition: Predicting the Need for Urgent Neonatal Balloon Atrial Septostomy

Greggory R. DeVore[1,2,3,6] · Gary Satou[4] · Mark Sklansky[4] · Bettina Cuneo[5]

Received: 9 November 2022 / Accepted: 13 February 2023 / Published online: 28 February 2023

Abstract

Introduction Speckle tracking analysis of the endocardium of the right (RV) and left (LV) ventricles was used to evaluate the size, shape, and contractility of these chambers in fetuses with D-Transposition of the great arteries (D-TGA) to identify fetuses that would require emergent balloon atrial septostomy (BAS) after birth.

Methods This was a retrospective analysis of fetuses with D-TGA and intact ventricular septum that were divided into 2 groups. Group 1 underwent urgent BAS after birth because of a restrictive atrial septum and group 2 did not. Using speckle tracking analysis, the end-diastolic and end-systolic RV and LV areas, lengths, widths, sphericity indices, and contractility were computed. Logistic regression analysis was performed to identify fetuses who would require urgent neonatal BAS.

Results Of the 39 fetuses with D-TGA, 55% ($n=22$) required urgent neonatal BAS (group 1) and 45% ($n=17$) (group 2) did not. When comparing D-TGA groups 1 and 2, differences were seen in RV and LV area, sphericity index for segment 1 of the LV, LV fractional area of change and free wall annular plane systolic excursion, fractional shortening for LV segment 12, and RV free wall strain. Regression analysis of these measurements identified 91% of neonates who underwent BAS, with a false-positive rate of 12%.

Conclusion Using speckle tracking analysis to evaluate the RV and LV, measurable differences were identified for the RV and LV size, shape, and contractility between fetuses who underwent neonatal urgent BAS vs. those who did not require this procedure.

Keywords Fetal echocardiography · D-Transposition of the great arteries · Congenital heart defect · Speckle tracking · Strain · Logistic regression · Balloon atrial septostomy

✉ Greggory R. DeVore
grdevore@gmail.com

1 Fetal Diagnostic Centers of Pasadena, Tarzana, and Lancaster, CA, USA

2 Division of Maternal-Fetal Medicine, Department of Obstetrics and Gynecology, David Geffen School of Medicine, UCLA, Los Angeles, CA, USA

3 Department of Obstetrics and Gynecology, Wayne State University, Detroit, MI, USA

4 Departments of Pediatrics and Obstetrics, The Heart Institute and the Colorado Fetal Care Center, Children's Hospital Colorado, University of Colorado School of Medicine, Aurora, CO, USA

5 Division of Pediatric Cardiology, Department of Pediatrics, UCLA Mattel Children's Hospital, David Geffen School of Medicine at UCLA, Los Angeles, CA, USA

6 Department of Obstetrics and Gynecology, David Geffen School of Medicine, UCLA, Suite 330, 50 Alessandro Place, Pasadena, CA 91105, USA

Introduction

D-Transposition of the great arteries (D-TGA) occurs in 1/3,413 live births and can have immediate and devastating complications following birth [1]. Because of the parallel pulmonary and systemic circulations, severe hypoxemia and death can occur rapidly if the atrial septum is restrictive, thus limiting the left to right atrial shunt bringing oxygenated blood to the aorta [2]. Balloon atrial septostomy (BAS), a bedside catheterization procedure, enlarges the patent foramen ovale and can be life-saving in newborns with a restrictive atrial septum [3]. While the prenatal detection of D-TGA has improved from 14 to 82% with the addition of the outflow tract and 3-vessel view screening of the fetal heart [4, 5] it is still difficult to predict those fetuses that will require BAS. Studies have concentrated on the atrial septum and the aneurysm of the fossa ovalis to risk stratify D-TGA fetuses, but results are variable [4–6]. No previous study has evaluated the size, shape, and contractility of the right and left ventricles between fetuses with D-transposition and fetuses with structurally normal hearts, as well as the differences within the D-transposition cohort that would predict the need for urgent neonatal BAS and improved pre-surgical outcomes.

The purpose of the current study was to evaluate the fetal D-TGA heart to (1) identify ventricular measurements that were significantly different between the control fetuses and those requiring neonatal BAS and those that did not undergo this procedure, (2) identify ventricular measurements that were significantly different between D-TGA fetuses that required urgent neonatal BAS from those that did not, and (3) derive a logistic regression equation that would predict the probability for urgent neonatal BAS that could be used in the prenatal clinical environment.

Materials and Methods

Normal Control Group

Two hundred normally grown fetuses with structurally normal hearts and without extracardiac defects were examined between 20 and 40 weeks of gestation and served as controls. Measurements from these fetuses have previously been reported with their corresponding sensitivities and specificities [6–13]. All measurements described in this communication were performed by one individual (GRD). The mean and standard deviation values from measurements of the right (RV) and left (LV) ventricles from 200 normal controls were normally distributed which allowed for the computation of z-score values of ventricular measurements in D-TGA fetuses. [6–13]

Study Fetuses: Prenatal Diagnosis of D-Transposition of the Great Arteries Neonatally Confirmed

This retrospective study was approved by the Colorado multiple institutional review board (IRB# 18-2384) and the University of California at UCLA (IRB# 16-000259). A search was conducted of the fetal cardiology databases of the Children's Hospital of Colorado and UCLA for fetuses with D-TGA and an intact ventricular septum: those with ventricular septal defects and other cardiovascular malformations were excluded. Digital Imaging and Communications in Medicine (DICOM) clips of the four-chamber view from the last examination prior to delivery were retrieved from the database. The criteria for urgent BAS were an oxygen saturation $< 70\%$ and a PO2 < 30 mmHg measured from the upper extremities in combination with a restrictive atrial shunt diagnosed by color Doppler echocardiography. D-TGA fetuses were divided into two groups: group 1 fetuses underwent urgent neonatal BAS within 24 h of birth and group 2 with an adequate atrial communication did not undergo BAS.

Right and Left Ventricular Endocardial Measurements Using Speckle Tracking Analysis

Two-dimensional images of the 4CV were imported into an offline cardiac software program (2D Fetal Cardiac Performance Analysis (2D CPA)), developed by TomTec Imaging Systems, Gmbh (Munich, Germany), using criteria for fetal applications that have been previously described [14]. The endocardial end-diastolic and end-systolic borders were defined using the quiver technique [15]. From 49 speckle tracking identified points distributed along the end-systolic and end-diastolic length of the ventricular endocardium, the pixel coordinates for each point were imported into a programed Excel spreadsheet that computed the measurements described below (Fig. 1).

Right and Left End-Diastolic Ventricular Size

From the 4-chamber view (Fig. 1A) the RV and LV end-diastolic area, mid-chamber length, and 24-segment transverse widths (Fig. 1B) were measured and regressed against gestational age as the independent variable to compute the corresponding D-TGA z-scores using equations of the mean and standard deviation previously published from the control group [11, 13].

Right and Left End-Diastolic Ventricular Shape

The 24-segment sphericity index was computed by dividing the end-diastolic length by each of the end-diastolic 24-segment widths (Fig. 1B) [12].

Right and Left Ventricular Contractility

Ventricular contractility was defined as non-volume measurements of the ventricles and categorized as follows: (1) global contractility, (2) longitudinal contractility, and (3) transverse contractility (Table 1). Global contractility was ascertained by measuring the fractional area change (Table 1, Fig. 2A) [8]. Longitudinal contractility was divided into two sections: (1) global, free, and septal wall longitudinal strain (Table 1, Fig. 2B–D) [6] and (2) free and septal wall annular plane systolic excursion (Table 1, Fig. 2E and F) [10]. Transverse contractility, defined as transverse fractional shortening, was computed for each of the 24-transverse width segments (Table 1, Fig. 2G). [7]

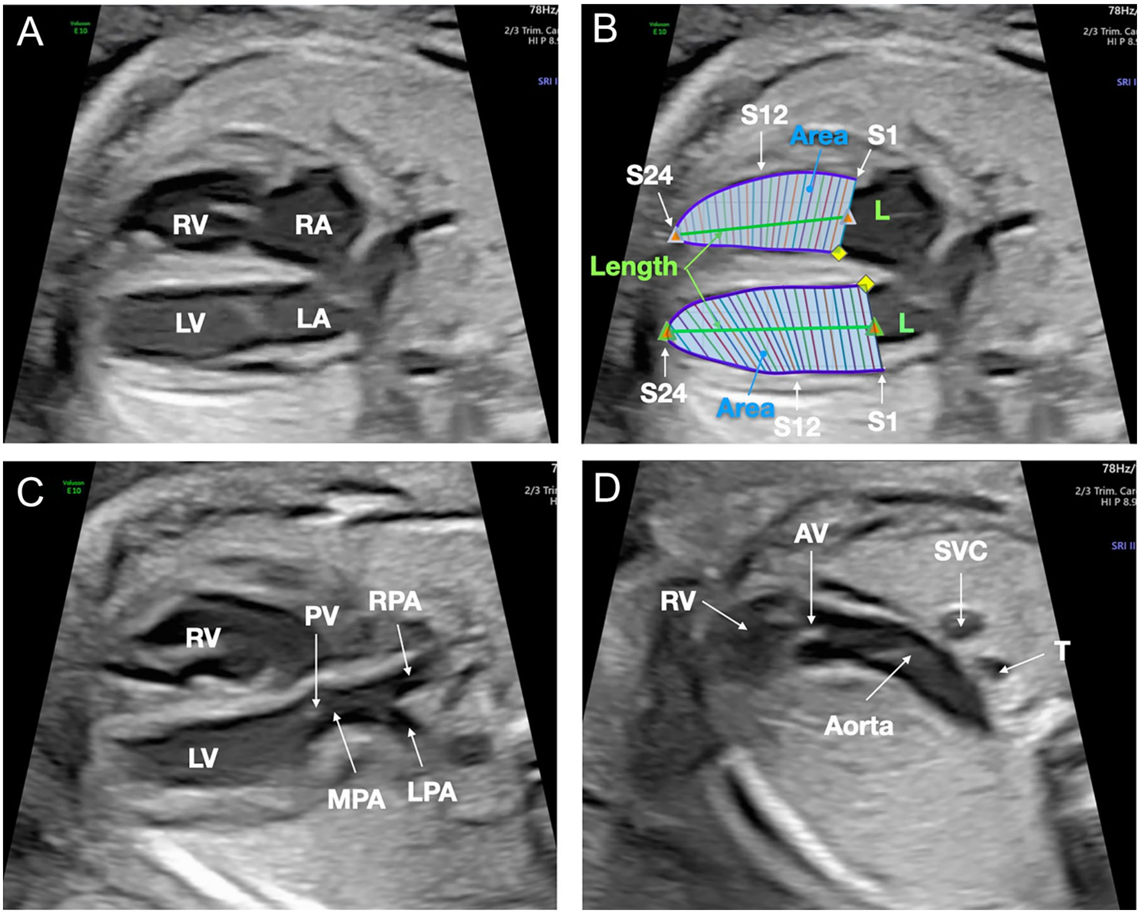

Fig. 1 End-Diastolic Measurements of the Size and Shape of the Right and Left Vernicles in a Fetus with D-Transposition. **A** Four-chamber view. **B** Measurements of the 24-segment transverse widths from the base (S1), mid-chamber (S12) and apex (S24, and the length (L). **C** Left outflow tract illustrating the main pulmonary originating from the left ventricle (LV). **D** Three-vessel tracheal view demonstrating the aorta originating from the right ventricle (RV). LA left atrium. RA right atrium, PV pulmonary valve, AV aortic valve, MPA main pulmonary artery, *RPA* right pulmonary artery, *LPA* left pulmonary artery, MPA, *SVC* superior vena cava, *T* trachea

Left Ventricular Function

Left ventricular function was defined as end-systolic and end-diastolic volume measurements of the LV computed using Simpson's rule which were derived from the 24-segment transverse widths and length measurements (Fig. 2H, Table 2) [9]. The volume measurements were used to compute the stroke volume, cardiac output, and the ejection fraction (Table 2) [9].

Statistical Analysis

All statistical analyses were performed using NCSS 21 (Kaysville, Utah, USA). The mean and standard deviation values from the 200 control fetuses for each of the measurements listed in Tables 1 and 2 were used to compute the z-score and equivalent centile for 39 fetuses with D-TGA, using gestational age as the independent variable (Eqs. 1 and 2).

$$z\text{-}score = \left(Measured\ Value_{D\text{-}TGA} - Mean_{Control\ Group}\right) / Standard\ Deviation_{Control\ Group}, \quad (1)$$

$$Excel\ Function\ to\ Compute\ Z\text{-}Score\ Centile = Normsdist(z\text{-}score\ value). \quad (2)$$

The computed z-scores for the D-TGA non-BAS and BAS fetuses were compared to 200 controls as well as to each other using the student *T* Test if the measurements were normally distributed or the Mann–Whitney U test if the measurements were not normally distributed.

Using the hierarchical forward selection protocol (NCSS 21, Kaysville, UT), logistic regression was performed to compute the probability of fetuses with D-TGA requiring neonatal BAS and those with D-TGA that did not require this procedure. The z-score value from each of the ventricular measurements identified from logistic regression was multiplied by its corresponding logistic regression coefficient

Table 1 Right and Left Ventricular Measurements of Contractility

Right and left ventricular measurements	Equation
Global contractility	
Fractional Area Change (Fig. 2A) [8]	[((end-diastolic area – end-systolic area)/end-diastolic area) × 100]
Longitudinal contractility: global strain	
Global longitudinal strain (Fig. 2 B) [6]	[((end-systolic endocardial length—end-diastolic endocardial length)/end -diastolic endocardial length) × 100]
Free wall strain (Fig. 2C) [18]	[((end-systolic endocardial free wall length – end-diastolic endocardial free wall length)/end-diastolic endocardial free wall length) × 100]
Septal wall strain (Fig. 2 D) [18]	[((end-systolic endocardial septal wall length – end-diastolic endocardial septal wall length)/end-diastolic endocardial septal wall length) × 100]
Longitudinal contractility: free wall and septal annular plane systolic excursion	
Free wall annular plane systolic excursion (Fig. 2F) [10]	[((free wall end-diastolic length measured from the apex to the annular base-free wall end-systolic length measured from the apex to the annular base)/ free wall end-diastolic length measured from the apex to the annular base) × 100]
Septal wall annular plane systolic excursion (Fig. 2F) [10]	[((septal wall end-diastolic length measured from the apex to the annular base—septal wall end-systolic length measured from the apex to the annular base)/ septal wall end-diastolic length measured from the apex to the annular base) × 100]
Transverse contractility	
24-Segment transverse fractional shortening (Fig. 2G) [7]	[((end-diastolic width – end-systolic width)/end-diastolic width) × 100]

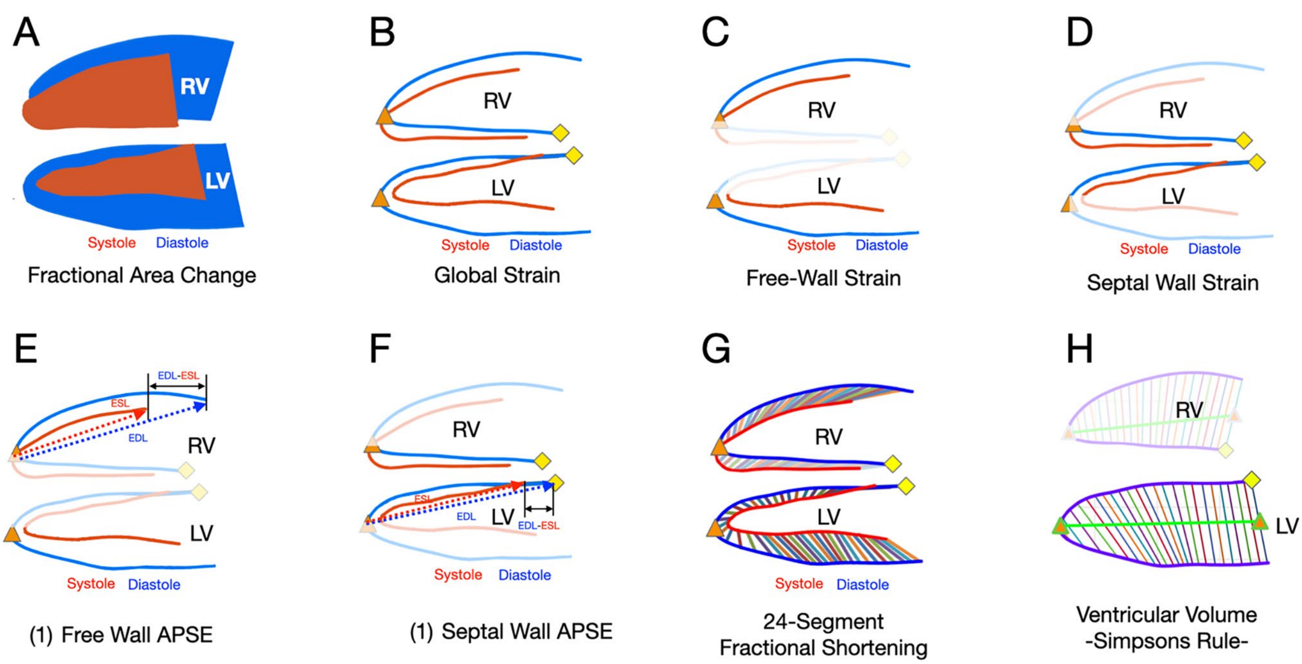

Fig. 2 Graphic illustrations of Ventricular Measurement Derived from Speckle Tracking Analysis of the Right and Left Ventricles. **A** Illustrates the systolic and diastolic areas used to compute the fractional area change. [8] **B**, **C**, and **D** Illustrate the global, free wall, and septal strain which are computed by measuring the endocardial end-systolic (red) and end-diastolic lengths (blue). [6] **E** and **F** Illustrate the measurements for computing the free wall and septal annular plane systolic excursion (APSE). **G** Illustrates the 24-segment fractional shortening measurement. **H** Illustrates the transverse width and length measurements used to compute the end-diastolic and end-systolic volumes using Simpson's Rule [9]

and the total summed for the identified variables to compute the Logit value. The Logit value was multiplied by *(1/(1 + 2.718^(-Logit)))* to compute the probability (> 50%) of a fetus with D-TGA requiring neonatal BAS.

Intraobserver and Interobserver Variabilities

The intraobserver variability reported in previous studies of ventricular area, length, and width measurements and

Table 2 Left Ventricular Function

Measurement	Equation
Left ventricular end-diastolic and end-systolic volumes (Fig. 2A) [9]	This was computed using Simpsons Rule from the 24-segment end-diastolic and end-systolic transverse width measurements and lengths.*
Left ventricular stroke volume [9]	[(end-diastolic volume) – (end-systolic volume)]
Left ventricular cardiac output [9]	(Heart rate x Stroke Volume)
Left ventricular ejection fraction [9]	[(end-diastolic volume) – (end-systolic volume)/end-diastolic volume] × 100

*The end-diastolic and end-systolic volumes were computed from the speckle tracking software by the Simpson method of disk analysis in which the area of each of the 24 segments is multiplied by each of the 24-segment lengths (between transverse segments) (Fig. 1A). [9]

ventricular contractility ranged between 0.93 and 0.98. [6–10] The interobserver variability between 2 examiners for measurements of ventricular size and contractility (GS and MS) was 0.97 [6–10]. Therefore, intraobserver and interobserver variabilities were not reported for the current study measuring the ventricles in the D-TGA fetuses since the same measurements have been previously validated for the control group.

Results

Demographics of Fetuses with D-Transposition of the Great Arteries

The last fetal echocardiogram performed prior to birth by the pediatric cardiologist was used for analysis. Fetuses with D-transposition ($n = 39$) were examined at a mean age of 29 weeks (range 20–37 weeks); 18 (46%) had their last fetal echo at < 32 weeks (range 19 6/7 to 31 0/7) of gestation. Neonatal BAS was performed in 22 newborns (55%) within 24 h of birth. Forty-one percent (7/17, range 20.9 to 29.7 weeks) of the non-BAS fetuses and 50% (11/22, range 19.6 to 31 weeks) of BAS fetuses were examined prior to 32 weeks of gestation.

End-Diastolic Size and Shape of the Right and Left Ventricles

Non-BAS Fetuses vs Controls

The end-diastolic LV length ($z = -1.58$; SD 1.4), RV length ($z = -1.03$; SD 1.14), and LV area ($z = -1.44$; SD 1.4) were significantly less ($P < 0.05$) than controls. The RV 24-segment end-diastolic width values were significantly less than controls for segment 16 of the mid-chamber and segments 17 to 24 for the apical chamber (Table 3). The LV transverse width segments 8–24 (mid- and apical chamber) were significantly less than controls (Table 4). The 24-segment SI measurements were significantly less than controls for the RV segments 1–11 (Table 5) and the LV segments 1–14 (Table 6), suggesting round or globular-shaped chambers.

BAS Fetuses vs Controls

There were no significant differences for the LV and RV end-diastolic areas and the LV length. However, the RV end-diastolic length ($z = -0.53$; SD 1.34) was significantly less ($P < 0.05$) than controls. There were no significant differences in the RV 24-segment end-diastolic widths when compared to controls except for the apical segments 22 to 24 (Table 3). All LV segment widths were significantly less than controls (Table 4). The 24-segment SI was significantly less than controls for segment 1 to 13 for the RV (Table 5), suggesting a globular-shaped chamber. However, for the LV all 24 segments had SI values greater than controls, suggesting a flattened chamber (Table 6).

Non-BAS vs BAS Fetuses

There was no significant difference between the non-BAS and BAS groups for the RV ($z = -0.54$; SD 1.6 vs -0.2; SD 1.43) and LV ($z = -1.44$; SD 1.4 vs -0.9; SD 1.35) areas or the RV length ($z = -1$; SD 1.14 vs -0.5; SD 1.34). However, the LV length of the non-BAS fetuses was significantly smaller ($z = -1.58$; SD 1.59 vs -0.17; AD 1.16) than the BAS fetuses. There were no significant differences for the 24-segment end-diastolic widths between the 2 groups for the RV (Table 3), and only a significant difference for segments 1 to 6 for the LV (Table 4), with the latter being smaller than the RV. There were no significant differences for the SI for all RV segments (Table 5). The 24-segment SI was significantly different between the two groups for all segments of the LV (Table 6).

Right and Left Ventricular Global and Longitudinal Contractility

Non-BAS Fetuses vs Controls

Table 7 lists the mean z-score values for the non-BAS fetuses which demonstrates the z-score values for the

Table 3 Z-score values for the right ventricle 24-segment end-diastolic transverse widths

Right ventricle segments	Non-BAS ($N=17$) vs controls Mean	SD	Z-score centile	*P*-value	BAS ($N=22$) vs controls Mean	SD	Z-score centile	*P*-value	Non-BAS vs BAS *P*-value
Base									
1	0.62	1.69	73%	0.11	0.55	1.66	71%	0.13	0.90
2	0.63	1.70	74%	0.11	0.61	1.67	73%	0.09	0.96
3	0.62	1.68	73%	0.12	0.65	1.64	74%	0.07	0.96
4	0.60	1.66	73%	0.14	0.68	1.62	75%	0.05	0.88
5	0.56	1.66	71%	0.20	0.70	1.61	76%	0.05	0.79
6	0.50	1.69	69%	0.29	0.71	1.63	76%	0.06	0.70
7	0.41	1.71	66%	0.62	0.70	1.65	76%	0.06	0.60
8	0.31	1.72	62%	0.72	0.67	1.67	75%	0.09	0.52
Mid									
9	0.21	1.73	58%	0.99	0.64	1.71	74%	0.12	0.45
10	0.11	1.72	54%	0.75	0.60	1.74	73%	0.18	0.39
11	0.01	1.70	50%	0.49	0.55	1.76	71%	0.28	0.33
12	− 0.10	1.69	46%	0.34	0.50	1.77	69%	0.47	0.29
13	− 0.20	1.67	42%	0.21	0.44	1.76	67%	0.45	0.26
14	− 0.30	1.64	38%	0.13	0.37	1.72	64%	0.59	0.23
15	− 0.35	1.66	36%	0.08	0.35	1.75	64%	0.74	0.21
16	− 0.45	1.63	33%	0.04	0.26	1.68	60%	0.93	0.19
Apical									
17	− 0.55	1.62	29%	0.0206	0.16	1.64	56%	0.81	0.18
18	− 0.69	1.56	24%	0.0399	− 0.02	1.53	49%	0.50	0.19
19	− 0.80	1.57	21%	0.0019	− 0.16	1.55	43%	0.25	0.21
20	− 0.86	1.55	19%	0.0007	− 0.30	1.58	38%	0.10	0.27
21	− 0.89	1.50	19%	0.0005	− 0.39	1.62	35%	0.05	0.32
22	− 0.89	1.46	19%	0.0004	− 0.44	1.65	33%	0.035	0.37
23	− 0.89	1.43	19%	0.0004	− 0.47	1.66	32%	0.028	0.40
24	− 0.89	1.42	19%	0.0005	− 0.48	1.66	32%	0.025	0.42

global contractility (FAC) of the RV and LV were significantly less than controls. For longitudinal contractility all values were significantly less than controls except for RV septal wall strain (Table 7).

BAS Fetuses vs Controls

When z-score values from BAS fetuses were compared to controls only the measurements of annular plane systolic excursion were significantly less than controls (Table 7).

Non-BAS vs BAS Fetuses

There were no significant differences between non-BAS and BAS fetuses for all global and longitudinal contractility measurements.

Left Ventricular Function

Non-BAS Fetuses vs Controls

Left ventricular stroke volume and ejection fraction z-score values were significantly lower than controls (Table 7).

BAS Fetuses vs Controls

Left ventricular stroke volume, cardiac output, and ejection fraction z-score values were significantly lower than controls (Table 7).

Table 4 Z-score values for the left ventricle 24-segment end-DIASTOLIC transverse widths

Left ventricle segments	Non-BAS ($N=17$) vs controls				BAS ($N=22$) vs controls				Non-BAS vs BAS P-value
	Mean	SD	Z-score centile	P-value	Mean	SD	Z-score centile	P-value	
Base									
1	− 0.14	0.71	44%	0.29	− 0.80	0.90	21%	< 0.001	0.02
2	− 0.14	0.72	45%	0.28	− 0.84	0.97	20%	< 0.001	0.01
3	− 0.13	0.76	45%	0.28	− 0.87	1.03	19%	< 0.001	0.01
4	− 0.13	0.81	45%	0.27	− 0.88	1.08	19%	< 0.001	0.02
5	− 0.15	0.85	44%	0.23	− 0.89	1.13	19%	< 0.001	0.03
6	− 0.21	0.88	42%	0.11	− 0.90	1.19	19%	< 0.001	0.04
7	− 0.28	0.91	39%	0.09	− 0.89	1.24	19%	< 0.001	0.10
8	− 0.37	0.96	36%	0.03	− 0.89	1.29	19%	< 0.001	0.17
Mid									
9	− 0.46	1.00	32%	0.02	− 0.89	1.34	19%	< 0.001	0.26
10	− 0.55	1.05	29%	< 0.01	− 0.90	1.37	18%	< 0.001	0.39
11	− 0.62	1.08	27%	< 0.01	− 0.92	1.38	18%	< 0.001	0.47
12	− 0.67	1.10	25%	< 0.01	− 0.94	1.39	17%	< 0.001	0.52
13	− 0.71	1.12	24%	< 0.01	− 0.97	1.39	17%	< 0.001	0.54
14	− 0.74	1.13	23%	< 0.01	− 0.99	1.38	16%	< 0.001	0.55
15	− 0.77	1.14	22%	< 0.001	− 1.01	1.38	16%	< 0.001	0.57
16	− 0.82	1.17	21%	< 0.001	− 1.04	1.40	15%	< 0.001	0.60
Apical									
17	− 0.89	1.22	19%	< 0.001	− 1.10	1.44	14%	< 0.001	0.63
18	− 1.00	1.30	16%	< 0.001	− 1.18	1.50	12%	< 0.001	0.71
19	− 1.14	1.39	13%	< 0.001	− 1.26	1.58	10%	< 0.001	0.79
20	− 1.22	1.45	11%	< 0.001	− 1.30	1.60	10%	< 0.001	0.86
21	− 1.24	1.45	11%	< 0.001	− 1.29	1.57	10%	< 0.001	0.91
22	− 1.23	1.43	11%	< 0.001	− 1.26	1.54	10%	< 0.001	0.94
23	− 1.22	1.41	11%	< 0.001	− 1.24	1.51	11%	< 0.001	0.95
24	− 1.21	1.41	11%	< 0.001	− 1.23	1.50	11%	< 0.001	0.96

Non-BAS vs BAS Fetuses

There were no significant differences in z-score values between non-BAS and BAS fetuses (Table 7).

Right and Left Ventricular 24-Segment Transverse Contractility

Non-BAS Fetuses vs Controls

Right ventricular fractional shortening z-score values were significantly less than controls for all mid-chamber and apical segments (Table 8). Left ventricular fractional shortening z-score values were significantly lower than controls for segments 12 to 16 of the mid-chamber and all apical segments (Table 9).

BAS Fetuses vs Controls

Only RV base segments 7 and 8, mid-chamber segments 9 and 10, and apical segments 23 and 24 were significantly less than controls (Table 8). For the LV, only apical segments 19 to 24 were significantly less than controls (Table 9).

Non-BAS vs BAS Fetuses

For the RV, there were significant differences between the 2 groups for segments 9 to 16 for the mid-chamber and segments 17 and 18 of the apical section (Table 8). For the LV there were no significant differences between the 2 groups for all 24 segments (Table 9).

Table 5 Right ventricular 24-segment sphericity index Z-score values

Right ventricle segments	Non-BAS ($N=17$) vs controls				BAS ($N=22$) vs controls				Non-BAS vs BAS *P*-value
	Mean	SD	Z-score centile	*P*-value	Mean	SD	Z-score centile	*P*-value	
Base									
1	− 0.98	1.04	16%	0.0002	− 0.61	0.85	27%	0.006	0.25
2	− 0.99	1.08	16%	0.0001	− 0.65	0.86	26%	0.004	0.27
3	− 0.99	1.14	16%	0.0001	− 0.67	0.88	25%	0.003	0.35
4	− 0.97	1.20	16%	0.0002	− 0.69	0.90	24%	0.002	0.40
5	− 0.94	1.27	17%	0.0004	− 0.69	0.92	24%	0.002	0.51
6	− 0.88	1.35	19%	0.02	− 0.68	0.96	25%	0.003	0.62
7	− 0.81	1.43	21%	0.00	− 0.66	1.00	26%	0.004	0.72
8	− 0.73	1.48	23%	0.01	− 0.63	1.04	27%	0.006	0.79
Mid									
9	− 0.67	1.50	25%	0.02	− 0.59	1.08	28%	0.021	0.85
10	− 0.61	1.51	27%	0.02	− 0.56	1.11	29%	0.015	0.90
11	− 0.56	1.49	29%	0.03	− 0.53	1.12	30%	0.021	0.94
12	− 0.51	1.48	31%	0.05	− 0.50	1.11	31%	0.029	0.98
13	− 0.45	1.46	32%	0.09	− 0.47	1.11	32%	0.041	0.98
14	− 0.40	1.43	35%	0.28	− 0.43	1.12	33%	0.06	0.94
15	− 0.34	1.39	37%	0.20	− 0.38	1.13	35%	0.09	0.91
16	− 0.28	1.36	39%	0.42	− 0.33	1.14	37%	0.14	0.89
Apical									
17	− 0.21	1.33	42%	0.42	− 0.28	1.13	39%	0.28	0.86
18	− 0.12	1.30	45%	0.64	− 0.21	1.10	42%	0.36	0.83
19	− 0.02	1.27	49%	0.94	− 0.11	1.05	46%	0.62	0.80
20	0.09	1.24	54%	0.72	0.00	1.01	50%	0.98	0.81
21	0.20	1.21	58%	0.45	0.13	1.04	55%	0.57	0.86
22	0.27	1.20	61%	0.30	0.23	1.12	59%	0.36	0.92
23	0.31	1.20	62%	0.23	0.30	1.21	62%	0.27	0.98
24	0.34	1.20	63%	0.19	0.35	1.28	64%	0.23	0.98

Logistic Regression Analysis Identifying Fetuses That Required Urgent Neonatal BAS

Logistic regression analysis identified 7 z-score measurements that correctly identified 91% (20/22) fetuses that required neonatal BAS, with a false-positive rate of 12% (2/17) (Table 10). The measurements identified from logistic regression included RV and LV area, LV sphericity index for segment 1, LV FAC, RV free wall strain, LV wall annular plane systolic excursion, and LV fractional shortening for segment 12. Supplement 1 lists the z-score values for each of the measurements identified using logistic regression equation, their corresponding logit values, and probability of requiring neonatal BAS for the 39 fetuses with D-TGA.

Clinical Implications

Review of the Pathophysiology of D-TGA

In an attempt to understand the underlying mechanisms that may explain the results from this study it would be important to review the physiological and anatomical consequences of D-TGA suggested by Rudolph in 2007 [16]. In the normal as well as D-TGA fetuses, oxygenated blood enters the RA from the ductus venosus and the left portal vein and preferentially streams across the foramen ovale to the LA [16]. Less oxygenated blood enters RA from the superior and inferior vena cava. In the normal fetus blood pumped from the RV, which contains lower O2 than

Table 6 Left ventricular 24-segment sphericity index Z-score values

Left ventricle segments	Non-BAS (N=17) vs controls				BAS (N=22) vs controls				Non-BAS vs BAS P-value
	Mean	SD	Z-score centile	p	Mean	SD	Z-score centile	P-value	
Base									
1	– 0.91	1	18%	< 0.001	0.47	0.97	68%	0.01	< 0.001
2	– 0.95	1.03	17%	0.002	0.51	1	69%	0.02	< 0.001
3	– 0.98	1.07	16%	< 0.001	0.557	1.1	71%	< 0.01	< 0.001
4	– 1	1.1	16%	< 0.001	0.59	1.17	72%	< 0.01	< 0.001
5	– 1	1.24	16%	< 0.002	0.61	1.24	73%	< 0.01	< 0.001
6	– 0.98	1.12	16%	< 0.001	0.64	1.28	74%	0.001	< 0.001
7	– 0.95	1.09	17%	< 0.001	0.65	1.32	74%	0.03	< 0.001
8	– 0.89	2.05	19%	< 0.002	0.67	1.34	75%	< 0.01	< 0.001
Mid									
9	– 0.84	1.01	20%	< 0.001	0.68	1.36	75%	< 0.01	< 0.001
10	– 0.78	0.97	22%	< 0.002	0.72	1.38	76%	0.O3	< 0.001
11	– 0.72	0.94	24%	0.007	0.76	1.4	78%	< 0.01	< 0.001
12	– 0.65	0.91	26%	0.01	0.08	1.42	53%	0.01	< 0.001
13	– 0.59	0.9	28%	0.01	0.85	1.43	80%	< 0.001	< 0.001
14	– 0.53	0.89	30%	0.03	0.89	143	81%	< 0.001	< 0.001
15	– 0.47	0.99	32%	0.06	0.93	1.42	82%	< 0.01	< 0.001
16	– 0.41	0.92	34%	0.1	0.99	1.42	84%	< 0.001	< 0.001
Apical									
17	– 0.32	0.96	37%	0.19	1.06	1.45	86%	< 0.001	< 0.001
18	– 0.22	1.03	41%	0.37	1.18	1.53	88%	< 0.001	< 0.001
19	– 0.2	1.12	42%	0.68	1.3	1.52	90%	< 0.001	< 0.001
20	0.02	1.12	51%	0.93	1.42	1.7	92%	< 0.001	< 0.001
21	0.13	1.29	55%	0.69	1.49	1.78	93%	< 0.001	< 0.01
22	0.2	1.34	58%	0.43	1.53	1.82	94%	< 0.001	< 0.02
23	0.24	1.37	59%	0.33	1.55	1.85	94%	< 0.001	< 0.02
24	0.27	1.39	61%	0.43	1.56	1.86	94%	< 0.001	< 0.02

the LV, is associated with constriction of the pulmonary vasculature and dilatation of the ductus arteriosus [16]. When D-TGA is present, the increased oxygen saturation present in the LV results in dilation of the pulmonary arteries and narrowing of the ductus arteriosus [16]. The increased pulmonary blood flow results in increased LA flow resulting in increased atrial pressure that may result in decreased flow through the FO [16]. Rudolph also noted that the above changes are most likely a 3rd trimester phenomena since increases in maternal oxygenation had no effect on pulmonary artery blood flow at 25–26 weeks of gestation but had a significant increase after 30 weeks of gestation [16, 17]. The above changes, depending upon their severity, are the precursors that may result in decreased flow through the FO following birth, thus comprising the newborn and requiring BAS.

Changes in Ventricular Size and Shape Between Non-BAS and Controls

We noted that the RV widths were significantly lower in the non-BAS fetuses for 1 mid and all apical segments of the ventricle (percentiles ranging between 19 and 33%) but the sphericity index was not abnormal. The reason for this was because the RV length was also significantly decreased when compared to controls, thus resulting in no significant change in the computed SI (length/width). For the base and mid-segments (9 to 11) the percentile widths, while not significant, ranged between the 50th and 74th centiles, resulting in decreased sphericity indices for these segments because of the decreased ventricular length. This would suggest a globular-shaped ventricle in the base and mid-segments of the RV chamber.

Table 7 Z-score values for right and left ventricular contractility and left ventricular function

Measurements	Non-BAS ($N=17$) vs Controls				BAS ($N=22$) vs Controls				Non-BAS vs BAS P-value
	Mean	SD	Z-score centile	P-value	Mean	SD	Z-score centile	P-value	
Global contractility									
RV fractional area change	– 1.49	2	7%	< 0.01	– 0.08	2.32	47%	0.81	0.05
LV fractional area change	– 1.07	1.80	14%	< 0.01	– 0.69	2.18	25%	0.05	0.56
Longitudinal contractility									
RV global strain	1.29	1.40	90%	< 0.01	0.42	2.00	66%	0.24	1.30
LV global strain	0.74	1.00	77%	< 0.01	0.19	1.70	58%	0.22	0.23
RV free wall strain	1.19	1.38	88%	< 0.01	0.15	1.87	56%	0.53	0.05
LV free wall strain	0.60	1.53	73%	0.02	– 0.11	1.63	46%	0.81	0.17
RV septal strain	0.52	1.56	70%	0.05	0.11	1.59	54%	0.63	0.43
LV septal strain	0.64	0.99	74%	0.01	0.32	1.47	63%	0.17	0.46
RV wall APSE	– 1.29	1.56	10%	< 0.01	– 0.62	1.00	27%	0.01	0.11
LV wall APSE	– 1.23	1.49	11%	< 0.01	– 0.54	1.30	29%	0.01	0.13
RV septal APSE	0.60	1.93	73%	0.03	1.41	1.28	92%	0.01	0.12
LV septal APSE	– 0.49	1.42	31%	< 0.01	– 0.33	1.00	37%	0.01	0.68
Left ventricular function									
Stroke volume	– 0.53	1.09	30%	0.02	– 0.78	5.78	22%	0.01	0.50
Cardiac output	– 0.51	1.11	31%	0.08	– 0.86	1.27	19%	0.01	0.37
Ejection fraction	– 1.04	1.89	15%	< 0.01	– 0.74	2.00	23%	0.01	0.64

RV right ventricle, *LV* left ventricle, *APSE* annular plane systolic excursion, *SD* standard deviation

Similar to the RV, the LV length and transverse widths, for segments 8 to 24 were significantly decreased when compared to controls (range 11 centile to 32 centile). However, because of the decreased LV length, the LV SI values were decreased for segments 1 to 14 of the LV, suggesting a globular-shaped chamber. The change to a globular shape of the RV and LV and often occurs with concomitant ventricular dysfunction associated with congenital heart defects. [12, 18, 19]

Changes in Ventricular Size and Shape Between BAS and Controls

The RV end-diastolic transverse widths were not significantly different than controls for segments 1 to 21, while the SI was significantly lower than controls for segments 1 to 13. This was the result of the decreased RV length, suggesting a globular-shaped RV base and mid-chamber.

Unlike the RV, all of the LV end-diastolic transverse widths were significantly lower than controls resulting in significantly greater SI values, suggesting a flattened LV chamber.

Changes in Ventricular Size and Shape Between Non-BAS and BAS Fetuses

All 24-segment RV transverse widths and SI measurements were not significantly different between the non-BAS and BAS fetuses. However, the BAS transverse widths were significantly lower for segments 1 to 7 at the base of the heart than the RV. This finding of a flattened LV chamber compared to the globular-shaped RV chamber may be attributed to be the result of decreased flow through the foramen ovale which is harbinger for the necessity of neonatal BAS.

Prior Studies Evaluating Ventricular Size and Shape in Fetuses with D-TGA

In 2020, Walter reported results of measurements of the ventricles in 21 fetuses with D-TGA using 2D ultrasound and noted an increased RV SI compared to the current study in which the SI was decreased [20]. In 2021, Patey examined 13 fetuses with D-TGA at term and reported findings that were similar to the current study which included RV and LV end-diastolic lengths to be decreased and the sphericity index of the RV to be more globular or round in shape [21]. Although conventical thinking has been that the ventricles imaged in the 4CV are "normal" in fetuses with D-TGA, our study and the study by Patey would suggest otherwise, with ventricular disproportion being a marker for fetuses at risk for D-TGA. [21]

Summary of Findings of Changes for Ventricular Contractility

In fetuses with D-TGA various combinations of the four types of contractility measurements (global contractility,

Table 8 Right ventricular 24-segment transverse fractional shortening Z-score values

Right ventricle segments	Non-BAS ($N=17$) vs controls				BAS ($N=22$) vs controls				Non-BAS vs BAS *P*-value
	Mean	SD	Z-score centile	*P*-value	Mean	SD	Z-score centile	*P*-value	
Base									
1	− 0.14	1.26	44%	0.89	0.22	1.49	59%	0.22	0.42
2	0.21	1.21	58%	0.28	− 0.36	1.29	36%	0.33	0.17
3	0.26	1.23	60%	0.24	− 0.26	1.31	40%	0.48	0.22
4	0.31	1.28	62%	0.26	− 0.13	1.35	45%	0.79	0.31
5	0.37	1.36	64%	0.15	0.04	1.40	51%	0.82	0.46
6	0.42	1.53	66%	0.11	0.24	1.50	59%	0.30	0.72
7	0.47	1.71	68%	0.08	0.49	1.59	69%	0.04	0.97
8	0.52	1.85	70%	0.06	0.75	1.65	77%	0.00	0.69
Mid									
9	− 1.04	2.61	15%	< 0.01	0.68	1.66	75%	0.01	0.02
10	− 1.24	2.59	11%	< 0.01	0.49	1.65	69%	0.04	0.02
11	− 1.36	2.47	9%	< 0.01	0.30	1.63	62%	0.22	0.02
12	− 1.41	2.31	8%	< 0.01	0.14	1.60	56%	0.57	0.02
13	− 1.42	2.14	8%	< 0.01	0.04	1.57	51%	0.89	0.02
14	− 1.38	1.98	8%	< 0.01	− 0.01	1.50	50%	0.95	0.02
15	− 1.30	1.84	10%	< 0.01	− 0.01	1.42	50%	0.94	0.02
16	− 1.24	1.74	11%	< 0.01	− 0.02	1.35	49%	0.96	0.02
Apical									
17	− 1.21	1.67	11%	< 0.01	− 0.06	1.33	47%	0.91	0.02
18	− 1.16	1.57	12%	< 0.01	− 0.15	1.31	44%	0.66	0.04
19	− 1.20	1.61	11%	< 0.01	− 0.28	1.43	39%	0.39	0.07
20	− 1.10	1.48	13%	< 0.01	− 0.40	1.39	34%	0.19	0.13
21	− 1.10	1.48	14%	< 0.01	− 0.54	1.41	29%	0.14	0.24
22	− 1.07	1.41	14%	< 0.01	− 0.65	1.32	26%	0.05	0.34
23	− 1.07	1.45	14%	< 0.01	− 0.70	1.34	24%	0.04	0.42
24	− 1.06	1.48	14%	< 0.01	− 0.73	1.34	23%	0.03	0.47

SD standard deviation

longitudinal global strain, annular plane systolic excursion, and transverse fractional shortening) occurred. When examining non-BAS vs BAS fetuses, only the non-BAS fetuses had abnormal global contractility and strain, while both groups had abnormal measurements of the annular plane systolic excursion. In addition, LV function (stroke volume, cardiac output, and ejection fraction) were decreased when compared to controls for the BAS group, with the non-BAS group having a normal cardiac output but abnormal stroke volume and ejection fraction. However, when comparing the non-BAS and BAS groups, there was no significant difference between the groups for any of the measurements listed in Table 7. These findings suggest that the RV in non-BAS fetuses demonstrates different types of contractility abnormalities (fractional area change and all strain measurements) than BAS fetuses. These measurements of the RV are not unexpected given the globular shape of the RV and has been observed in fetuses with growth restriction and other fetal abnormalities. [10, 22, 23]

Prior Studies Evaluating Ventricular Contractility in Fetuses with D-TGA

In the study by Patey they used pulsed Doppler and speckle tracking to measure systolic ventricular function and found LV CO to be decreased in fetuses with D-TGA, [21] and Walter reported two measurements that were contrary to the findings reported in the current study: an increased LV CO vs decreased LV CO and increased LV ejection fraction vs decreased LV ejection fraction [20]. The decreased LV SV, CO, and EF in BAS fetuses is concordant with the decreased transverse widths of the 24 segments and decreased length of the LV noted in the current study.

Table 9 Left ventricular 24-segment transverse fractional shortening Z-score values

Left ventricle segments	Non-BAS (*N* = 17) vs controls				BAS (*N* = 22) vs controls				Non-BAS vs BAS *P*-value
	Mean	SD	Z-score centile	*p*	Mean	SD	Z-score centile	*P*-Value	
Base									
1	0.22	1.21	59%	0.15	− 0.37	1.28	36%	0.73	0.15
2	0.22	1.18	59%	0.17	− 0.33	1.26	37%	0.77	0.17
3	0.21	1.18	58%	0.19	− 0.29	1.26	39%	0.83	0.22
4	0.18	1.24	57%	0.48	− 0.25	1.31	40%	0.45	0.31
5	0.17	1.26	57%	0.30	− 0.14	1.30	44%	0.97	0.46
6	0.15	1.28	56%	0.45	0.00	1.26	50%	0.79	0.72
7	0.07	1.39	53%	0.70	0.09	1.29	53%	0.61	0.97
8	− 0.06	1.54	48%	0.94	0.13	1.37	55%	0.50	0.69
Mid									
9	− 0.21	1.64	42%	0.56	0.13	1.44	55%	0.50	0.50
10	− 0.35	1.66	36%	0.26	0.07	1.47	53%	0.66	0.41
11	− 0.49	1.63	31%	0.11	− 0.02	1.47	49%	0.96	0.37
12	− 0.60	1.59	28%	0.04	− 0.11	1.46	45%	0.73	0.33
13	− 0.68	1.54	25%	0.02	− 0.18	1.45	43%	0.53	0.30
14	− 0.76	1.50	22%	0.01	0.19	1.45	58%	0.47	0.24
15	− 0.81	1.44	21%	< 0.01	− 0.19	1.47	42%	0.47	0.20
16	− 0.84	1.39	20%	< 0.01	− 0.20	1.50	42%	0.44	0.18
Apical									
17	− 0.85	1.33	20%	< 0.01	− 0.25	1.53	40%	0.31	0.21
18	− 0.86	1.28	20%	< 0.01	− 0.37	1.57	35%	0.13	0.31
19	− 0.84	1.22	20%	< 0.01	− 0.52	1.57	30%	0.03	0.49
20	− 0.86	1.21	20%	< 0.01	− 0.69	1.61	25%	0.01	0.72
21	− 0.83	1.18	20%	< 0.01	− 0.78	1.60	22%	< 0.01	0.92
22	− 0.81	1.16	21%	< 0.01	− 0.84	1.59	20%	< 0.01	0.95
23	− 0.80	1.15	21%	< 0.01	− 0.87	1.58	19%	< 0.01	0.87
24	− 0.79	1.15	21%	< 0.01	− 0.89	1.58	19%	< 0.01	0.83

SD standard deviation

Table 10 Logistic regression coefficients used to compute the probability of neonatal urgent BAS

Independent variables	Regression coefficient	Standard error	Lower 95% confidence limit	Upper 95% confidence limit	Odds ratio
Intercept	1.5743	0.9491	− 0.2859	3.4345	4.82738
Ventricular end-diastolic size and shape					
LV area	− 1.63242	0.93291	− 3.46089	0.19604	0.19546
RV area	− 1.0044	0.70423	− 2.38466	0.37586	0.36626
LV sphericity index segment 1	6.51899	2.66673	1.29229	11.7457	677.89613
Ventricular contractility					
LV Fractional area change	1.88771	0.96727	− 0.00811	3.78353	6.6042
RV Free wall strain	− 0.8802	0.45977	− 1.78133	0.02094	0.4147
LV wall annular plane systolic excursion	0.8533	0.65265	− 0.42587	2.13246	2.34738
LV fractional shortening segment 12	− 4.3942	1.97728	− 8.2696	− 0.51881	0.01235

LV left ventricle, *RV* right ventricle

Predicting the Need for Neonatal BAS Using Speckle Tracking Analysis

The logistic regression analysis identified measurements of RV and LV area and LV shape as well as 4 measurements of ventricular function that had a sensitivity of 91% with false-positive rate of 12%. Review of the logistic regression analysis in Supplement 1 demonstrates that using the above measurements all fetuses less than 32 weeks were identified as having a high probability for requiring neonatal BAS. Therefore, the current approach is not dependent on changes in the fetal heart manifesting during the 3rd trimester of pregnancy.

Prior Studies Predicting the Need for Neonatal BAS

In 2011, Punn examined 26 fetuses with D-TGA, of which 54% required BAS and reported evaluation of abnormal movement of the FO and reverse flow of the DA having sensitivities ranging between 31 and 64%. [24] In 2017, Vigneswaran evaluated 40 fetuses with D-TGA and measured the total atrial septal length (TSL) and foramen ovale (FO) length and reported that a FO/TSL < 0.5 had a sensitivity of 99%, but a false-positive rate of 40% [25] In 2021 Patey reported the following measurements that had a sensitivity of 86%, with a false-positive rate as high as 17%: RV/LV end-diastolic area ratio, pulmonary valve/aortic valve dimension ratio, RV/LV cardiac output ratio, and the foramen ovale length/

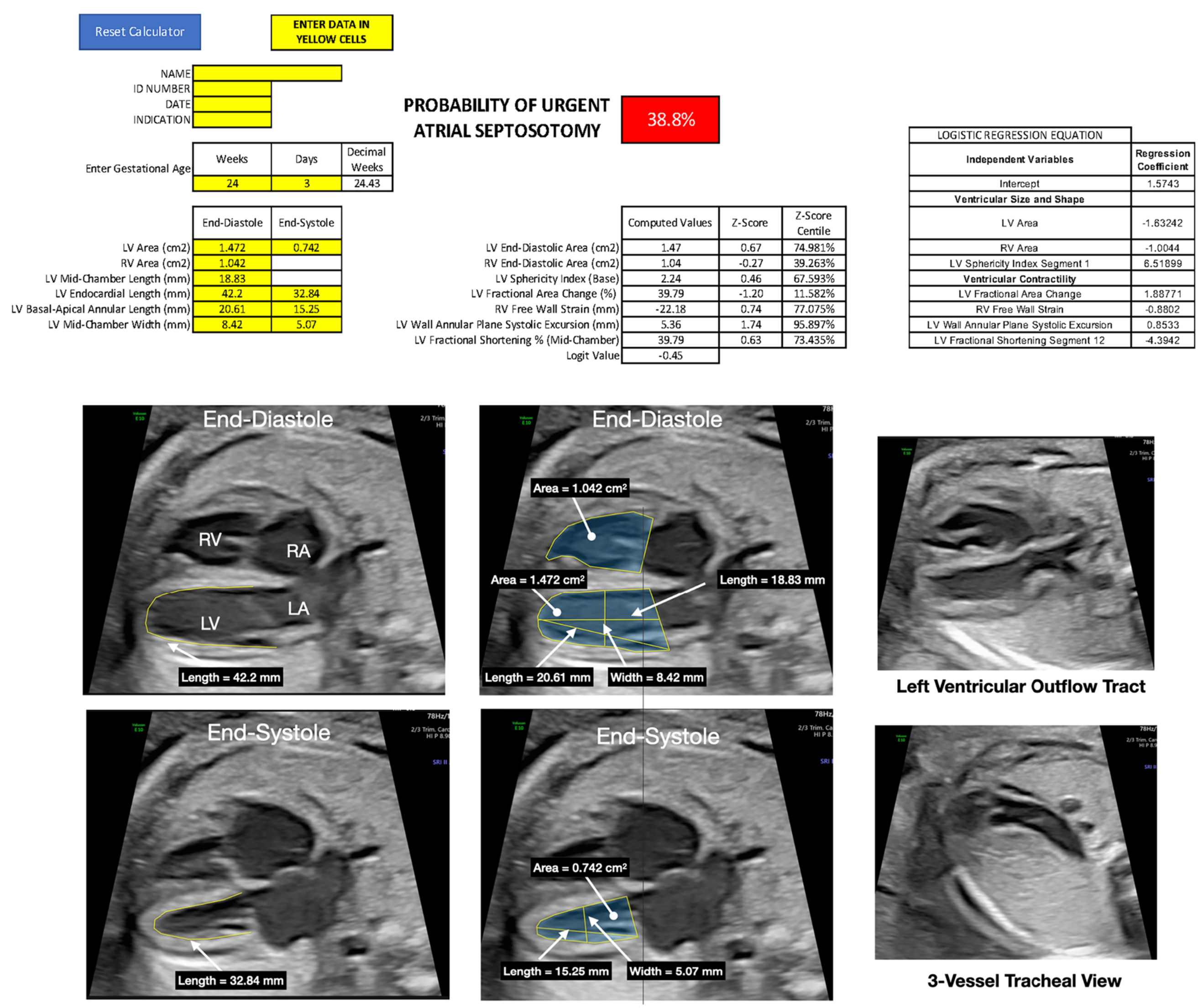

Fig. 3 Calculator to compute the probability of requiring a neonatal urgent BAS. To use the calculator the user enters the gestational age and measurements illustrated below the calculator. Once entered the z-scores and probability are calculated. The clear the calculator of the measurements and computed values, the user clicks the blue button "Reset Calculator." *RV* right ventricle, *LV* left ventricle, *LA* left atrium, *RA* right atrium

total interatrial septal length ratio [21]. In 2021, Della Gatta reported that a length of the foramen ovale of > 6.5 mm, measured within 3 weeks of delivery, had a sensitivity of 100% but a false-positive rate of 43%. In 2021 Masci evaluated 31 fetuses with D-TGA using 5 measurements of the atrial septum to predict urgent BAS and found none of the measurements predicted the need for urgent treatment [26].

Therefore, prior studies using various measurements of the atrial chambers, size of the FO, and measurement of pulsed Doppler blood flow through the DA have reported wide variations of sensitivities varying between 0 and 100% with false-positive rates as high as 43%.

Research Implications

This study provides clinical information with a probability calculator to identify fetuses with D-TGA who may be at risk for neonatal BAS, a life-saving procedure. The probability calculator could be used to evaluate fetuses in future with D-TGA to validate the usefulness of this approach. The benefit of the current approach is that it can be applied to fetuses between 20 and 32 weeks, a time in which changes in the size of the foramen ovale may be manifested.

Strengths and Limitations

The strength of this study, we believe, is the simplicity in which ventricular measurements derived from speckle tracking analysis can be generated from a single 4-chamber view in less than 5 min. The measurements in Table 10, used to compute the probability for requiring neonatal BAS, can be obtained using the length, width, and area measurements available on all fetal ultrasound machines. Supplement 2 is an Excel spreadsheet (Fig. 3) that provides a calculator with images describing the measurements to compute the probability of requiring urgent neonatal BAS. Limitations of the study include its retrospective nature and that not all fetuses were evaluated in the 3rd trimester when the pathophysiology of the abnormal measurements should be most obvious. Prospective evaluation of fetuses with D-TGA will be beneficial to test the Excel calculator developed from these study results.

Conclusion

This study applied speckle tracking analysis of the RV and LV, in fetuses with D-TGA, and found that measurements from the 4-chamber view may help identify which fetuses are likely to require urgent neonatal BAS.

Supplementary Information The online version contains supplementary material available at https://doi.org/10.1007/s00246-023-03131-y.

Author Contributions All authors contributed to design, analysis, and writing of the manuscript.

Funding This study was not supported by any funding or grants.

Declarations

Conflict of interest The authors report no conflict of interest.

References

1. Mai CT, Isenburg JL, Canfield MA et al (2019) National population-based estimates for major birth defects, 2010–2014. Birth Defects Res 111(18):1420–1435. https://doi.org/10.1002/bdr2.1589
2. Liebman J, Cullum L, Belloc NB (1969) Natural history of transpositon of the great arteries. Anatomy and birth and death characteristics. Circulation 40(2):237–62. https://doi.org/10.1161/01.cir.40.2.237
3. Mukherjee D, Lindsay M, Zhang Y et al (2010) Analysis of 8681 neonates with transposition of the great arteries: outcomes with and without Rashkind balloon atrial septostomy. Cardiol Young 20(4):373–380. https://doi.org/10.1017/s1047951110000296
4. Everwijn SMP, van Nisselrooij AEL, Rozendaal L et al (2018) The effect of the introduction of the three-vessel view on the detection rate of transposition of the great arteries and tetralogy of Fallot. Prenat Diagn 38(12):951–957. https://doi.org/10.1002/pd.5347
5. Ravi P, Mills L, Fruitman D et al (2018) Population trends in prenatal detection of transposition of great arteries: impact of obstetric screening ultrasound guidelines. Ultrasound Obstet Gynecol 51(5):659–664. https://doi.org/10.1002/uog.17496
6. DeVore GR, Klas B, Satou G, Sklansky M (2017) Longitudinal annular systolic displacement compared to global strain in normal fetal hearts and those with cardiac abnormalities. J Ultrasound Med. https://doi.org/10.1002/jum.14454
7. DeVore GR, Klas B, Satou G, Sklansky M (2017) Twenty-four segment transverse ventricular fractional shortening: a new technique to evaluate fetal cardiac function. J Ultrasound Med. https://doi.org/10.1002/jum.14455
8. DeVore GR, Klas B, Satou G, Sklansky M (2019) Quantitative evaluation of fetal right and left ventricular fractional area change using speckle-tracking technology. Ultrasound Obstet Gynecol 53(2):219–228. https://doi.org/10.1002/uog.19048
9. DeVore GR, Klas B, Satou G, Sklansky M (2019) Evaluation of fetal left ventricular size and function using speckle-tracking and the simpson rule. J Ultrasound Med 38(5):1209–1221. https://doi.org/10.1002/jum.14799
10. DeVore GR, Klas B, Satou G, Sklansky M (2019) Speckle tracking of the basal lateral and septal wall annular plane systolic excursion of the right and left ventricles of the fetal heart. J Ultrasound Med 38(5):1309–1318. https://doi.org/10.1002/jum.14811
11. DeVore GR, Klas B, Satou G, Sklansky M (2017) Evaluation of the right and left ventricles: an integrated approach measuring the area, length, and width of the chambers in normal fetuses. Prenat Diagn 37(12):1203–1212. https://doi.org/10.1002/pd.5166
12. DeVore GR, Klas B, Satou G, Sklansky M (2017) The 24-segment sphericity index: a new technique to evaluate fetal cardiac

diastolic shape. Ultrasound Obstet Gynecol. https://doi.org/10.1002/uog.17505
13. DeVore GR, Cuneo B, Klas B, Satou G, Sklansky M (2019) Comprehensive evaluation of fetal cardiac ventricular widths and ratios using a 24-segment speckle tracking technique. J Ultrasound Med 38(4):1039–1047. https://doi.org/10.1002/jum.14792
14. DeVore GR, Polanco B, Satou G, Sklansky M (2016) Two-dimensional speckle tracking of the fetal heart: a practical step-by-step approach for the fetal sonologist. J Ultrasound Med 35(8):1765–1781. https://doi.org/10.7863/ultra.15.08060
15. DeVore GR, Satou G, Sklansky M (2021) Comparing the non-quiver and quiver techniques for identification of the endocardial borders used for speckle-tracking analysis of the ventricles of the fetal heart. J Ultrasound Med 40(9):1955–1961. https://doi.org/10.1002/jum.15561
16. Rudolph AM (2007) Aortopulmonary transposition in the fetus: speculation on pathophysiology and therapy. Pediatr Res 61(3):375–380. https://doi.org/10.1203/pdr.0b013e318030d5b9
17. Rasanen J, Wood DC, Debbs RH, Cohen J, Weiner S, Huhta JC (1998) Reactivity of the human fetal pulmonary circulation to maternal hyperoxygenation increases during the second half of pregnancy: a randomized study. Circulation 97(3):257–262. https://doi.org/10.1161/01.cir.97.3.257
18. DeVore GR, Haxel C, Satou G et al (2021) Improved detection of coarctation of the aorta using speckle-tracking analysis of fetal heart on last examination prior to delivery. Ultrasound Obstet Gynecol 57(2):282–291. https://doi.org/10.1002/uog.21989
19. DeVore GR, Satou GM, Afshar Y, Harake D, Sklansky M (2021) Evaluation of fetal cardiac size and shape: a new screening tool to identify fetuses at risk for tetralogy of fallot. J Ultrasound Med 40(12):2537–2548. https://doi.org/10.1002/jum.15639
20. Walter C, Soveral I, Bartrons J et al (2020) Comprehensive functional echocardiographic assessment of transposition of the great arteries: from fetus to newborn. Pediatr Cardiol 41(4):687–694. https://doi.org/10.1007/s00246-019-02279-w
21. Patey O, Carvalho JS, Thilaganathan B (2021) Urgent neonatal balloon atrial septostomy in simple transposition of the great arteries: predictive value of fetal cardiac parameters. Ultrasound Obstet Gynecol 57(5):756–768. https://doi.org/10.1002/uog.22164
22. DeVore GR, Zaretsky M, Gumina DL, Hobbins JC (2017) Abnormal cardiovascular 24-segment sphericity index of the right and left ventricles in fetuses with growth restriction. Ultrasound Obstet Gynecol. https://doi.org/10.1002/uog.18820
23. DeVore GR, Gumina DL, Hobbins JC (2019) Assessment of ventricular contractility in fetuses with an estimated fetal weight less than the tenth centile. Am J Obstet Gynecol 221(5):498.e1-498.e22. https://doi.org/10.1016/j.ajog.2019.05.042
24. Punn R, Silverman NH (2011) Fetal predictors of urgent balloon atrial septostomy in neonates with complete transposition. J Am Soc Echocardiogr 24(4):425–430. https://doi.org/10.1016/j.echo.2010.12.020
25. Vigneswaran TV, Zidere V, Miller OI, Simpson JM, Sharland GK (2017) Usefulness of the prenatal echocardiogram in fetuses with isolated transposition of the great arteries to predict the need for balloon atrial septostomy. Am J Cardiol 119(9):1463–1467. https://doi.org/10.1016/j.amjcard.2017.01.017
26. Masci M, Pasquini L, Alsaied T et al (2021) Reliability of fetal echocardiography in predicting postnatal critical hypoxia in patients with transposition of great arteries and intact ventricular septum. Pediatr Cardiol 42(7):1575–1584. https://doi.org/10.1007/s00246-021-02642-w